Molecular Vision 2025; 31:231-243 <http://www.molvis.org/molvis/v31/231>
Received 12 December 2023 | Accepted 6 September 2025 | Published 8 September 2025

Unravelling γD-crystallin aggregation pathway to understand cataract formation using fluorescence correlation spectroscopy

Mangesh Bawankar,[1] Bhaswati Sengupta,[2] Sujata Malik,[1] Pratik Sen,[3] Ashwani K. Thakur[1]

[1]Department of Biological Sciences and Bioengineering, Mehta Family Centre for Engineering in Medicine, Indian Institute of Technology, Kanpur, UP India; [2]Department of Cancer Biology and Genetics. The Ohio State University, Columbus, OH; [3]Department of Chemistry, Indian Institute of Technology, Kanpur, UP India

Purpose: To characterize the aggregation behavior of the γD-crystallin protein in an acidic environment with a focus on the formation of intermediate species. The research employs fluorescence correlation spectroscopy to unravel the intricate molecular events leading to aggregation, contributing to a comprehensive understanding of cataract formation.
Methods: The kinetics of γD-crystallin protein aggregation were studied with a reversed-phase high-performance liquid chromatography sedimentation assay, a ThT binding assay, and light scattering. We used fluorescence correlation spectroscopy (FCS) to recognize intermediate aggregate species and characterized them with Fourier transform infrared spectroscopy (FTIR). Further, the morphologic characterization of aggregates was done by transmission electron microscopy (TEM), and their hydrophobic characteristics were analyzed using the 8-anilino-1-naphthalenesulfonic acid binding assay.
Results: A negligible lag phase was observed in the aggregation kinetic experiments of the γD-crystallin protein. Pentamer, 25-mer, and higher oligomer intermediates were formed on the aggregation pathway. Conformation studies by FCS and FTIR have shown that oligomers are rich in cross-β sheet and random coil structure; however, they constitute more α-helix and less cross-β sheet structure than fibrils. TEM analysis revealed the approximate size of oligomers (diameter ~10 nm), protofibrils (~15 nm), and fibrils (~15 to ~35 nm).
Conclusions: In this study, we reported the presence of various intermediate aggregate species formed on the aggregation pathway of γD-crystallin protein at low pH. This will open new areas of research in understanding the detailed aggregation mechanism and aggregation hotspot within unfolded γD-crystallin monomers. The insights gained will also pave the way for future research in the realm of amyloid formation in cataract.

Cataract is an eye disease in which crystallin proteins lose their native structure and aggregate in the lens fiber cells [1]. Mature lens fiber cells do not possess any protein synthesis and degradation machinery. Therefore, crystallins must be maintained in the native conformation for their long-term functioning in the lens [2]. Human γD-crystallin is an important protein in the context of cataract disease. Proteins such as γD-crystallin [3,4], lysozyme [5,6], and bovine serum albumin (BSA) [7] may require incubation with acidic pH, high temperature, or the presence of denaturants to form amyloid fibrils in vitro. The pH of an eye lens of a healthy individual is in the range of 6.8 to 7.2 [8,9]. γD-crystallin does not aggregate under this pH range. However, it is suggested that in diabetic conditions, increased glucose level leads to anaerobic conversion of glucose to lactic acid in the lens tissue, which may result in acidic pH [10]. The presence of a low level of oxygen in the lens nucleus may create anaerobic conditions and leads to the accumulation of lactic acid [10]. Second, an acidic environment in lysosomes may also play an important role in the formation of amyloid fibrils during degradation of improperly folded γD-crystallin protein in early stages of lens development. These amyloid fibrils may act as seeds for sequestering γD-crystallin protein in the matured lens fiber cells to start the aggregation pathway toward cataract formation [11].

Although the detailed mechanism of aggregation of γD-crystallin protein is still not known, earlier reports have shown that γD-crystallin and its N-terminal domain (NTD) and C-terminal domain (CTD) form amyloid fibrils under acidic conditions [11]. By using two-dimensional infrared (IR) spectroscopy, Moran et al. have reported that under acidic conditions, CTD of the γD-crystallin protein is an important region for nucleation and elongation of fibril growth [12]. The same group in a subsequent study has stated that CTD forms the amyloid core of the γD-crystallin fibrils under acidic pH [13]. However, the presence of intermediate aggregate species on the aggregation pathway to amyloid formation and their structural details are not known. In many amyloid-forming proteins and polypeptides, oligomers are initial intermediate

Correspondence to: Ashwani K Thakur, Department of Biological Sciences and Bioengineering, Mehta Family Centre for Engineering in Medicine, Gangwal School of Medical Sciences and Technology, Indian Institute of Technology, Kanpur, UP India-208016; Phone: +91-512-259-4077; email: akthakur@iitk.ac.in

species on the pathway of amyloid fibril formation [14,15]. Moreover, in some neurodegenerative diseases, oligomers were more toxic than amyloid fibrils [15,16]. Also, these initial aggregates may act as the template for the growth of higher-order aggregate species. In some amyloid diseases, it was observed that different oligomers' sizes, conformation, and concentrations have different effects on the cells. For example, in the case of Alzheimer's disease, Aβ oligomers were reported to have an affinity for cell membranes, synaptic contacts, and the activation of the mitochondrial apoptotic death pathway [17]. Similarly, in Parkinson's disease, it was observed that different oligomer species of α-synuclein have different effects on cells. For example, one type of oligomers increases cell permeability and causes cell death while others enter through the cell membrane and act as a seed to form amyloid fibrils [18]. Thus, the same might be possible in the case of cataract formation. Although the toxicity of oligomers may not be as important as that of neurodegenerative diseases, their interactions with cell membranes or effect on different cell pathways during lens development could have a role in the progression of cataract. Due to the heterogeneity of the aggregating system and the transient nature of intermediate species in the aggregation pathway, it is challenging to study these intermediate species. However, recent advances in single-molecule detection techniques, like fluorescence correlation spectroscopy (FCS), allow researchers to determine size and oligomer species formed during protein aggregation. Hence, in this study, aggregation behavior of γD-crystallin protein was monitored under acidic conditions to study the aggregation mechanism, with an emphasis on intermediate species formation during amyloid formation.

METHOD

Materials and chemicals: Isopropyl β-D-1-thiogalactopyranoside (IPTG) and trifluoroacetic acid (TFA) were purchased from Sisco Research Laboratories (Mumbai, Maharashtra, India). Sodium chloride, sodium monobasic phosphate, sodium dibasic phosphate, and acetonitrile were purchased from Merck (Rahway, NJ). Thioflavin T (ThT) and 7-Diethylamino-3-(4'-Maleimidylphenyl)-4-Methylcoumarin (CPM) were purchased from Sigma-Aldrich (St. Louis, MO). Lysogeny broth (LB) media and the dialysis bag were purchased from Himedia (Maharashtra, India), and a 100-kDa centrifugal filter was purchased from Amicon Millipore (Bedford, MA).

Protein purification: We received plasmids containing the human γD-crystallin gene from Prof. Martin Zanni (Department of Chemistry, University of Wisconsin-Madison, WI) as a gift. The human γD-crystallin gene was cloned in expression vector pET-16b [12,13]. Recombinant plasmid was transformed in the BL21DE3 (pLys) strain. Next, recombinant bacteria were streaked on an LB-agar plate containing ampicillin and incubated at 37 °C overnight. The next day, a single colony from the plate was picked and added to 10 ml LB broth containing ampicillin. This was incubated at 37 °C with shaking at 175 rpm overnight. Then, this culture was added to 1 liter LB broth containing ampicillin and incubated at 37 °C with shaking at 175 rpm until optical density (OD) reached 0.6. Culture was induced with 1 mM IPTG and allowed to grow for the next 4 h. Cells were collected by centrifugation at 3,470 rcf, 4 °C for 15 min (Sorvall Lynx 6000 ×g centrifuge, Thermo Fisher, Waltham, MA). Next, the cell pellet was suspended in binding buffer (20 mM phosphate buffer, 100 mM NaCl, 0.01% sodium azide, 10 mM imidazole, pH 7) and lysed by probe sonication (repeated cycle of 20 s on, 40 s off for 30 min). Cell debris was separated by centrifugation at 10,400 rcf at 4 °C for 30 min (Sorvall Lynx 6000 ×g centrifuge). Supernatant containing soluble protein was applied on a Ni-NTA (QIAGEN, Hilden, Germany; 5 ml) column by using a peristaltic pump. Then, protein was eluted with a linear gradient of elution buffer (20 mM phosphate buffer, 100 mM NaCl, 0.01% sodium azide, 500 mM imidazole, pH 7). Next, the protein was dialyzed with dialysis buffer (20 mM phosphate buffer, 100 mM NaCl, 2 mM EDTA, 0.01% sodium azide, pH 7) for 12 h at room temperature, replacing the old buffer with the new buffer every 3 h. After dialysis, protein was centrifuged at 139,600 rcf (Sorvall MTX 150) at 4 °C for 1 h before using. The protein purity was checked using sodium dodecyl sulfate–polyacrylamide gel electrophoresis (Appendix 1). Nucleotide sequence of the γD-crystallin gene was confirmed by plasmid sequencing (SciGenom Labs, Kochi, Kerala, India).

Determination of protein concentration: The concentration of γD-crystallin protein was determined by taking OD at 280 nm on a NanoDrop (ND-100, Themo Fisher) spectrophotometer. Protein concentration was calculated by the Beer-Lambert law for which the extinction coefficient of 42,860 $M^{-1}cm^{-1}$ at 280 nm (calculated by using ExPASy's ProtParam tool) was used. For the 8-anilino-1-naphthalenesulfonic acid (ANS) binding assay and tryptophan fluorescence assay, the concentration of γD-crystallin protein, oligomers, and fibrils was determined by the BCA method. Each species was solubilized in 8 M urea and heated at 70 °C until dissolved before performing the BCA method.

Spontaneous aggregation kinetics by reversed-phase high-performance liquid chromatography sedimentation assay, light scattering, and thioflavin binding assay: Reversed-phase high-performance liquid chromatography (RP-HPLC)

sedimentation, light scattering, and thioflavin (ThT) binding assays were performed to understand aggregation kinetics of γD-crystallin protein in pH 2.5. RP-HPLC was used to calculate percent monomers at different time points of aggregation reaction. Percent monomer was calculated by dividing the area under the peak at respective time points with the peak area at the zero time point, and the obtained value was multiplied by 100 [19]. A curve was generated by plotting percent monomers versus time. From this curve, information on different phases of aggregation reaction was derived [19]. Sedimentation assay was performed using the RP-HPLC system (Agilent Technologies, Santa Clara, CA; 1260 Infinity system) connected with the reverse-phase C18 column (Eclipse plus, 3.5 µM, 4.6 × 100 mm; Agilent Technologies). The γD-crystallin protein at 30 µM was incubated at 37 °C in dialysis buffer (20 mM phosphate buffer, 100 mM NaCl, 2 mM EDTA, 0.01% sodium azide) in pH 2.5. From the reaction mixture, an 80 µl sample was taken at different time points and centrifuged at 139,600 rcf (Sorvall MTX 150) at 4 °C for 30 min. Then, 40 µl of supernatant was collected and mixed with 10 µl of dialysis buffer (pH 7), and 2 µl of it was injected in the RP-HPLC. Protein was eluted by using an increasing gradient of acetonitrile containing 0.05% TFA. The absorbance of the protein was monitored at 215 nm.

To perform light scattering and ThT binding assays, γD-crystallin protein at 30 µM was incubated in dialysis buffer (20 mM phosphate buffer, 100 mM NaCl, 2 mM EDTA, 0.01% sodium azide, pH 2.5) at 37 °C. Then, 140 µl of the sample was collected at each time point, and light scattering was monitored on the LS-55 spectrofluorometer (Perkin Elmer, Waltham, MA) at 450 nm (excitation and emission slit width 5 nm). To this solution, ThT (52 µM) was added, and fluorescence was monitored on the same instrument at a 450 nm excitation and 489 nm emission wavelength using the excitation and emission slit width of 5 nm and 10 nm, respectively.

Fluorescence correlation spectroscopy: The γD-crystallin protein was tagged with a fluorescent molecule CPM (7-diethylamino-3-(4′-maleimidylphenyl)-4-methylcoumarin). CPM binds covalently with the solvent-exposed free cysteine residue of the protein. Tagging was performed by mixing γD-crystallin protein (60 µM) in dialysis buffer (20 mM phosphate buffer, 100 mM NaCl, 2 mM EDTA, 0.01% sodium azide, pH 7) [20,21] with CPM dye (48 µM) at a 1:0.8 ratio in the dark under continuous stirring conditions for 12 h. Volume of reaction was 5 ml. After 12 h of stirring, CPM-tagged protein was centrifuged at 139,600 rcf (Sorvall MTX 150) at 25 °C for 1 h and immediately used to study aggregation kinetics. Tagged protein can be stored at −20 °C after flash freezing in liquid nitrogen. Tagged protein was diluted to 30 µM in dialysis buffer (pH 7). The pH of the sample was lowered to 2.5 by adding HCl, and aggregation was induced by incubating the reaction mixture at 37 °C. Samples were collected at different time points of ongoing aggregation reaction, diluted to 40 nM, and placed on a coverslip on the sample platform of the FCS setup. FCS setup is based on an inverted optical microscope (IX-71; Olympus, Tokyo, Japan) equipped with 60X water immersion objective with 1.2 NA. A 5-mW, 405-nm laser source 19T was used to excite the sample. The detailed description of the setup can be found in our previous publications [22,23]. Focal point distance was kept at 40 µm from the upper surface of a coverslip. The emitted photons were collected and autocorrelated using the correlator card and displayed using the laboratory view program on a computer. The measured fluorescence intensity autocorrelation data, , can be expressed as [24]:

$$G(\tau) = \frac{(\delta F(t)\delta F(t+\tau))}{?(F(t))^2}$$

where is the average fluorescence intensity, and and are the fluctuations in the fluorescence intensity around the mean value at time and , respectively, and are given by and . The Autocorrelation function arising from the diffusion is given by [24]:

$$G(\tau) = \frac{1}{N}\left(1 + \frac{\tau}{\tau_D}\right)^{-1}\left(1 + \frac{\omega^2\tau}{\tau_D}\right)^{-\frac{1}{2}}\left(1 + ae^{-\frac{\tau}{\tau_R}}\right)$$

In the above equation, is the number of particles in the observation volume and (i.e., the ratio of the radial and axial radii of the three-dimensional Gaussian volume). Here, is the time component of any additional process than the diffusion, and is its amplitude. In the case of a two-component system (protein monomers and oligomers) governing the diffusion, the above equation will be modified as

$$G(\tau) = \frac{1}{(N_1+N_2)^2}\left\{N_1\left(1 + \frac{\tau}{\tau_{D1}}\right)^{-1}\left(1 + \frac{\omega^2\tau}{\tau_{D1}}\right)^{-\frac{1}{2}} + N_2\left(1 + \frac{\tau}{\tau_{D2}}\right)^{-1}\left(1 + \frac{\omega^2\tau}{\tau_{D2}}\right)^{-\frac{1}{2}}\right\}\left(1 + ae^{-\frac{\tau}{\tau_R}}\right)$$

The translational diffusion coefficient and the hydrodynamic radius can be calculated from the measured diffusion time and the radius of the observation volume () [25].

$$D_t = \frac{r^2}{4\tau_D}$$

Radius (*r*) of the observation volume was estimated from the diffusion time () of rhodamine 6G in water (= 4.14 *10^{-6} cm^2 s^{-1}) at 298 K following the standard procedure [25]. The transverse radius and the observation volume were calculated to be 292 nm and 0.6 fl, respectively. The hydrodynamic radius (r_H) of the protein was determined from the diffusion coefficient () using the Stokes-Einstein equation as

$$r_H = \frac{k_B T}{6\pi D_t}$$

where is the Boltzmann constant, is the absolute temperature (298 K in the present study), and is the viscosity of the medium.

Transmission electron microscopy: The γD-crystallin protein (30 µM) was incubated at 37 °C in dialysis buffer (20 mM phosphate buffer, 100 mM NaCl, 2 mM EDTA, 0.01% sodium azide, pH 2.5). Then, 5 µl of the sample was collected at each time point of the ongoing aggregation reaction and adsorbed for 2 min on the carbon-coated 200-mesh copper grids (electron microscopy). Grids were washed with MQ water, and samples were stained with 2% uranyl acetate and viewed on a TECNAI 200 kV TEM (FEI; Electron Optics, West Orange, NJ) instrument. Dimensional analysis of oligomer and fibrils was done using ImageJ software version 1.47 (National Institutes of Health, Bethesda, MD) from different grids imaged. For fibrils, the width of fibrils was measured at three different positions, and the average width was reported for one fibril.

Purification of oligomeric species volume of reaction: The γD-crystallin protein (30 µM) was incubated at 37 °C in dialysis buffer (20 mM phosphate buffer, 100 mM NaCl, 2 mM EDTA, 0.01% sodium azide, pH 2.5) for 1.5 h to form oligomers. Then, samples were divided equally into three 1.5 ml Eppendorf tubes and incubated at 37 °C, 25 °C, and 10 °C, respectively. Here, we wanted to slow down the aggregation reaction after 1.5 h, that is, after oligomer formation (result of transmission electron microscopy [TEM] analysis) so that oligomers could be purified without converting to aggregates. As explained below, maximum time required for oligomer purification is 2 h at 25 °C or 10 °C. Thus, aggregation reaction was monitored by the RP-HPLC sedimentation assay for 2 h. For oligomer purification, γD-crystallin protein (30 µM, 5 ml) was incubated at 37 °C in dialysis buffer, pH 2.5, for 1.5 h to generate oligomers. We performed all oligomer purification steps at 10 °C. This reaction mixture was then loaded on a 100-kDa centrifugal filter at 10 °C to retain species more than 100 kDa. Then, species retained above the centrifugal filter (300 µl) were washed by passing a 5 ml dialysis buffer (pH 2.5) three times through the same centrifugal filter. Further, these purified species were centrifuged at 16,000 ×g (Eppendorf 5417R) for 20 min at 10 °C to remove higher aggregates if any. The concentration of purified oligomers obtained after purification was 3 µM.

ANS and tryptophan fluorescence assay: ANS dye at 35 µM was incubated with γD-crystallin monomers, oligomers, and fibrils at room temperature for 10 min in the dark. The concentration of each of these species was 0.65 µM. Fluorescence of dye was monitored from 400 to 700 nm using an excitation wavelength of 380 nm. Excitation and emission slit width was 10 nm. For tryptophan fluorescence, γD-crystallin monomers, oligomers, and fibrils at 0.68 µM each in dialysis buffer (20 mM phosphate buffer, 100 mM NaCl, 2 mM EDTA, 0.01% sodium azide, pH 2.5) were used to monitor change in tryptophan fluorescence. Tryptophan was excited at 295 nm, and emission was monitored from 300 to 500 nm with an excitation and emission slit width of 10 nm. The volume of sample used in both assays was 140 µl.

Fourier transform infrared spectroscopy: Fourier transform infrared spectroscopy (FTIR) spectra were recorded on a Bruker Tensor 27 FTIR instrument (Bruker Optics, Billerica, MA). Measurements were done by loading 30 µl γD-crystallin protein (25 µM) in dialysis buffer (20 mM phosphate buffer, 100 mM NaCl, 0.01% azide, 2 mM EDTA) on a BioATR II cell equipped with an mercury cadmium telluride (MCT) detector under continuous purging of nitrogen gas. For a good signal-to-noise ratio, 120 scans were collected at 4 cm^{-1} resolution. Baseline correction from wavenumber 1,600 to 1,700 cm^{-1} was done by using the rubber band correction method [26]. The number of baseline points used was 64. The secondary derivative was calculated using 9 smoothing points, and all peaks from wavenumber 1,600 to 1,700 cm^{-1} were considered for secondary structure quantification. Further, deconvolution of the original absorbance spectra was done by using the Levenberg-Marquardt method in the curve fit option of OPUS version 7 software [26]. All peaks corresponding to different secondary structure wavenumbers were set to peak maxima of original absorbance spectra. Width for all the peaks was set to 10. Further, an autofit tab was used to get integral values for each peak. Percentage of secondary structures was calculated by dividing integral values of the wavenumber that corresponded to a particular secondary structure to the sum integral values of all these wavenumbers.

RESULTS

Aggregation kinetics of γD-crystallin protein: RP-HPLC sedimentation assay, light scattering, and ThT binding assay were performed simultaneously with ongoing aggregation reaction. A decrease in percent monomers and therefore an increase in aggregation was observed in the RP-HPLC sedimentation assay; this signifies γD-crystallin protein undergoes aggregation under the experimental conditions (Figure 1, black line). An increase in the light scattering was observed as the aggregation progressed, indicating the appearance of larger-size assembly formation during the aggregation reaction (Figure 1, blue line). Simultaneously, an increase in ThT binding indicates that an amyloid-like structure is present in the aggregates of γD-crystallin formed at pH 2.5 (Figure 1, red line) from the beginning and throughout the aggregation reaction. The detection of oligomers of γD-crystallin protein has revealed the existence of cross-β sheet structures. Consequently, ThT exclusively interacts with these structures when they are in the oligomeric state, leading to its binding being evident from the early stages of the aggregation process. Further, methods like FCS and analytical ultracentrifugation (AUC) are used to determine the size of aggregates formed at different time points of the ongoing aggregation reaction.

Characterization of initial aggregating species: FCS was performed to know the size of aggregates formed during the initial stages of the aggregation reaction. Autocorrelation curves were recorded at different time points of tagged γD-crystallin protein, and diffusion times were calculated

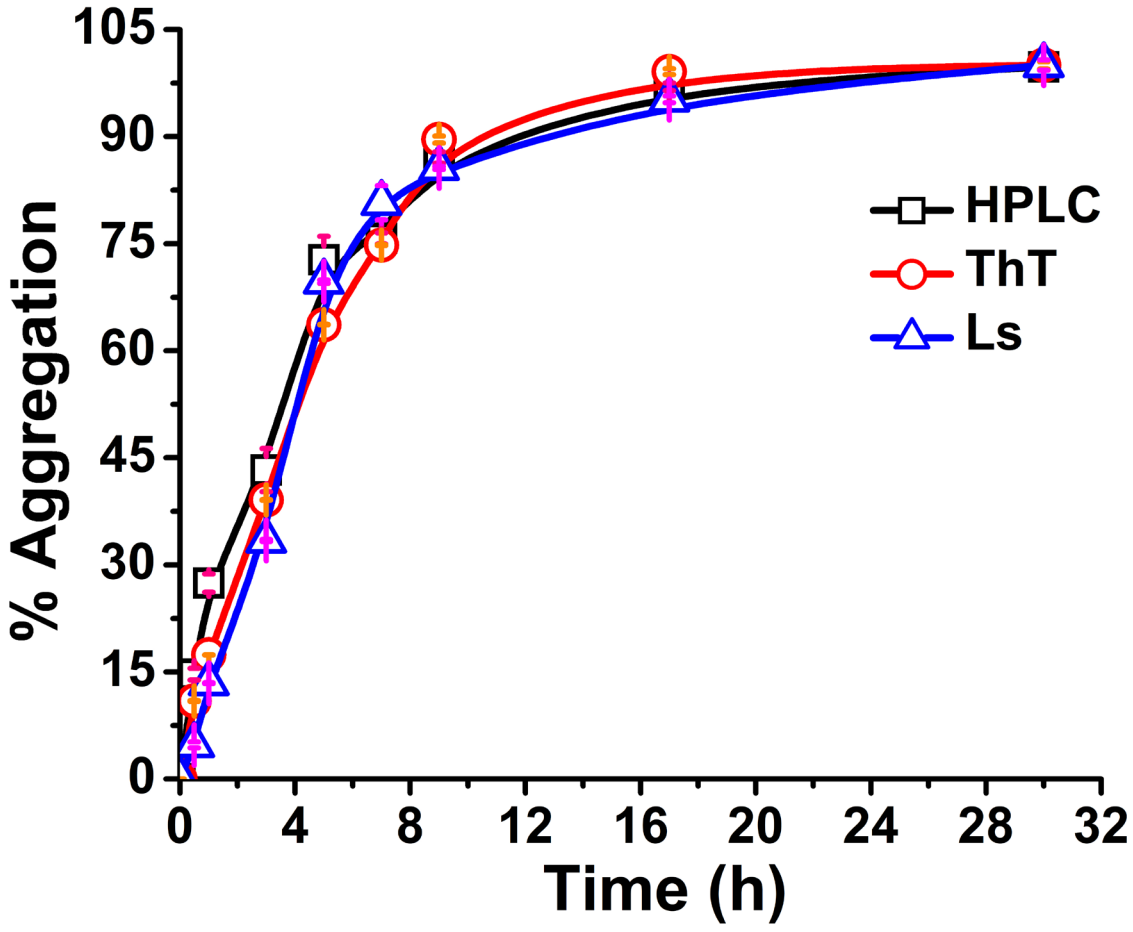

Figure 1. Aggregation kinetics of γD-crystallin protein at pH 2.5. The black line represents the RP-HPLC sedimentation assay, the red line represents the Thioflavin-T (ThT) binding assay, and the blue line represents the light scattering of γD-crystallin. In the RP-HPLC sedimentation assay, the percentage of monomers was converted into the percentage of aggregates, while the intensity values of light scattering and the ThT binding assay were normalized, considering the intensity value at 18 h as 100%.

using equations (2) and (3) (Methods). Before conducting an experiment, it was important to ensure the monomeric state of γD-crystallin protein at pH 2.5. Therefore, size of the γD-crystallin protein (hydrodynamic radius) in the beginning of the aggregation reaction (Figure 2) was compared with the value obtained at pH 7 (Appendix 1). Size of the γD-crystallin protein obtained at pH 2.5 was slightly more than pH 7. This might be due to change in the conformation of protein under acidic conditions. Next, molecular weight was calculated from analytical ultracentrifugation analysis of γD-crystallin protein at pH 7 and found to be 22.96 kDa, which corresponds to monomeric mass of the protein. To know the approximate number of monomeric species present at pH 2.5 before the reaction starts, volume ($v=4/3\pi r^3$) as calculated from the size considering spherical shape of the protein. Then the volume obtained was divided by the one found at pH 7. After these calculations, a value of 1.32 was obtained (Appendix 1), which indicates CPM-tagged γD-crystallin protein is present as a monomer before the start of the aggregation reaction. Therefore, a one-state component equation (equation (2), Methods) was used to determine the diffusion time of the monomers at 0 h before the start of the aggregation reaction. For all other time points, a two-state component equation was used (equation (3), Methods). The radius of the intermediate species formed during the aggregation reaction was observed to be gradually increasing as the aggregation progressed (Figure 2A). To know the approximate number of monomers in the aggregates formed at different time points of the aggregation reaction, the volume of aggregates was divided by the volume of the monomer at 0 h obtained at pH 2.5. At 0 h, only monomers are present; therefore, we used a single-component equation (equation (2)) to determine the radius. However, from 3 min onward, aggregate assemblies start forming; hence, we used a two-state component equation (equation (3)) to determine the diffusion time of intermediate species. FCS data indicate that on the aggregation pathway of γD-crystallin protein under pH 2.5, an aggregate species constituting approximately 5 ± 0.66 monomers was formed after 3 min (Appendix 1). As the aggregation reaction progressed, the aggregates gradually grew by the addition of more monomeric units or association of lower aggregate species. At 6 min, aggregate species constituted approximately 25 monomers. At 12 min, aggregate species containing approximately 110 ± 82 monomers were observed. At later time points, as the aggregation progressed, higher oligomer species were formed (Figure 2A).

Characterization of aggregates by TEM: Morphology of the aggregates formed during aggregation of γD-crystallin was studied by TEM. Spherical particles (oligomers) having a diameter of ~10 nm were observed after 1.5 h of the aggregation reaction. More images showing the presence of oligomers are given in (Appendix 2). No fibril like structures were seen at this time point. Predominantly, protofibrils having a width of ~7 nm were observed after 3 h of aggregation reaction. After 5 and 30 h, fibrils like structures having a width of ~15 nm and ~35 nm were observed (Figure 3).

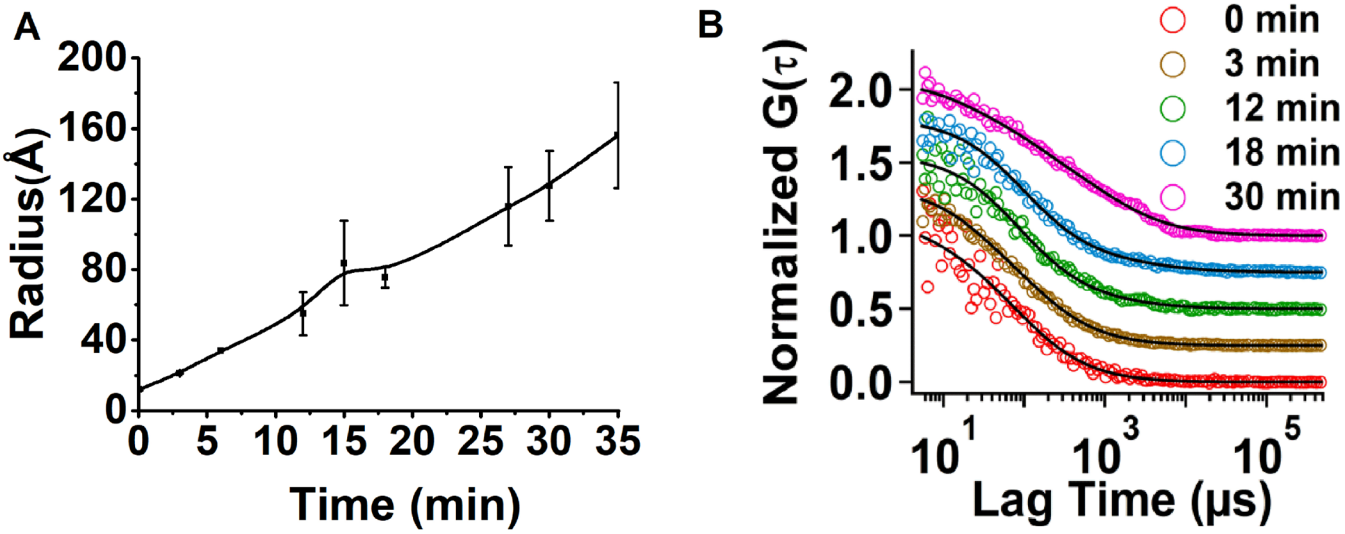

Figure 2. Fluorescence correlation spectroscopy (FCS) analysis of γD-crystallin protein aggregation at pH 2.5. **A**: The radius of the aggregation intermediates formed during the aggregation pathway at pH 2.5, calculated using diffusion time with equations 4 and 5. **B**: Best-fit lines (black) of autocorrelation curves (circles) representing aggregate species at different time points. To avoid overcrowding of data, the FCS traces for 6 min, 27 min, and 35 min are not shown.

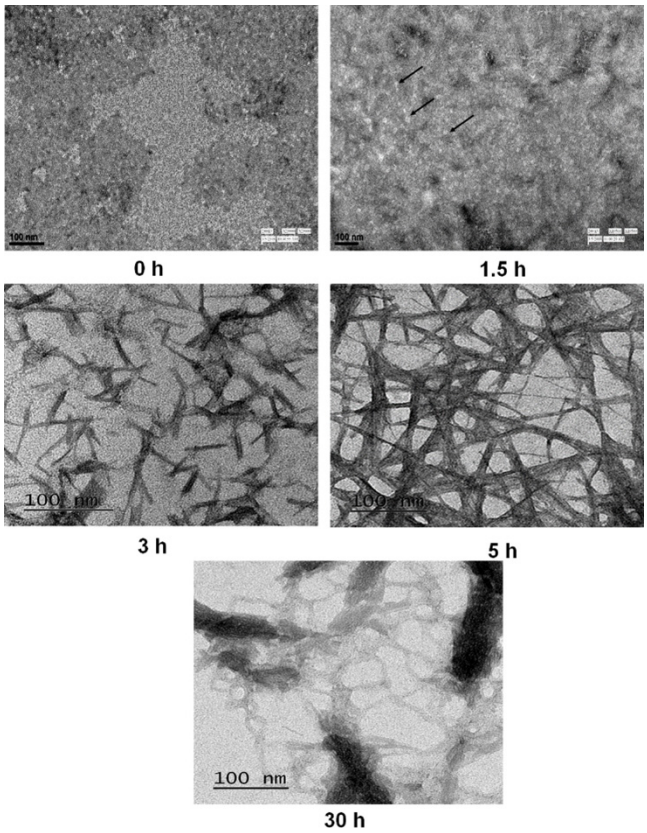

Figure 3. Transmission electron microscopy (TEM) images of γD-crystallin aggregation at different time points during the aggregation reaction. Oligomers were observed at 1.5 h (indicated by the black arrow), which grew to form protofibrils at 3 hours and fibrils at 5 h and 30 h. The scale bar represents 100 nm.

Change in hydrophobic characteristics of the aggregates: FCS data showed that as the aggregation of γD-crystallin progressed, various intermediate species, with increasing radius, were formed at pH 2.5. TEM analysis represents morphology of the intermediate species formed at the different time points of the aggregation reaction differing in size and shape. It is possible that these aggregating intermediates may have different biophysical characteristics than γD-crystallin monomers. Change in the conformation of γD-crystallin protein monomers, oligomers, and fibrils was studied by tryptophan fluorescence and the ANS binding assay. TEM analysis performed on the aggregation reaction in acidic pH showed that the oligomers were formed at 1.5 h of the aggregation reaction. At this point, □65−70% monomers were present in the reaction mixture, as revealed by the RP-HPLC sedimentation assay (Figure 1). Hence, it might be challenging to perform a protein conformation study of oligomers under these conditions since the presence of remaining γD-crystallin monomers in the aggregation reaction may interfere in the assay. Therefore, to characterize oligomers, remaining monomers after the formation of oligomers were removed. To achieve this, the aggregation reaction was slowed down with a lower temperature. The RP-HPLC sedimentation assay indicated the aggregation reaction had decelerated at 25 °C and 10 °C (Figure 4A). Oligomer purification was achieved as discussed in the Methods. A dynamic light scattering (DLS) experiment suggested that the size of purified oligomers was 94 ± 1 nm (Appendix 2).

Tryptophan fluorescence is one of the measures to determine the structural dynamics of a protein molecule [27]. Tryptophan fluorescence intensity of γD-crystallin monomers, oligomers, and fibrils was examined. Red shift in the wavelength showing maximum fluorescence intensity was observed in oligomers (352 ± 2 nm) and fibrils (349 ± 1nm) as compared to monomers (340 ± 2 nm; Figure 4B). This suggests that the environment of the tryptophan changes in oligomers and fibrils. Next, change in protein conformation was also studied by the ANS binding assay [28]. ANS dye binds to exposed hydrophobic patches of a protein and shows the increase in fluorescence intensity with a blue shift [28]. A blue shift was observed in the wavelength corresponding to maximum fluorescence intensity after binding

of the dye to oligomers (503 ± 1 nm) and fibrils (497 ± 1 nm) as compared with γD-crystallin monomers (527 ± 1 nm; Figure 4C). This shows the exposure of hydrophobic residues of γD-crystallin protein in oligomers and fibrils. In protein aggregation, various species are formed at different times of the aggregation reaction by the addition of monomers and/or the association of lower species to form higher-order species. γD-crystallin is a globular protein, and in its native structure, hydrophobic patches are present inside the protein structure. But, as the aggregation progresses, γD-crystallin protein loses its native structure. This leads to change in tryptophan environment and exposure of more hydrophobic patches.

Secondary structure analysis of γD-crystallin aggregates: The secondary structures of γD-crystallin are studied using FTIR spectroscopy. In the monomeric state, the FTIR analysis has shown that monomers at pH 7 mostly consist of β-sheet (1,630–1,637 cm^{-1}) and β-turn (1,662–1,678 cm^{-1} and 1,689–1,699 cm^{-1} for β-turn type I and type II, respectively). As the pH is decreased to 2.5, the β-sheet (1,630–1,637 cm^{-1}) remains as it is, whereas the β-turn changes its seems to form an α-helix (1,647–1,662 cm^{-1}; Appendix 3). Separation of oligomers from the remaining monomers was performed as explained in the Methods. Further, we have used these purified oligomers to determine their secondary structures by FTIR spectroscopy. FTIR analysis showed that oligomers and fibrils of γD-crystallin consist of cross-β sheet (1,620 cm^{-1} for oligomers, 1,618 cm^{-1} for fibrils), random coil (1,641 cm^{-1} for oligomers, 1,642 cm^{-1} for fibrils), α-helix (1,659 cm^{-1} for oligomers, 1,659 cm^{-1} for fibrils), and β-turn (1,675 cm^{-1}, 1,693 cm^{-1} for oligomers and 1,673 cm^{-1}, 1,693 cm^{-1} for fibrils) structures. However, structural contents varied in both species (Figure 5, Appendix 3). In oligomers, the main peak of the β-sheet present (1,630 cm^{-1}) in the γD-crystallin protein monomers shifted to a lower wavenumber, which is characteristic of the cross-β sheet structure [29,30]. It can be inferred that oligomers are rich in the cross-β sheet structure. These results were corroborated with the binding of ThT dye to the aggregates (Figure 1, red). In addition, oligomers were found to contain more α-helix and approximately the same random coil and β-turn contents as compared to fibrils (Figure 5). Also, lesser content of the cross-β sheet was present in the oligomers than in the fibrils. Hence, FTIR analysis showed that oligomers, although small in size, have common structural features with fibrils but possess distinct secondary structural characteristics other than γD-crystallin monomers. A circular dichroism (CD) experiment suggested that oligomers were rich in β-sheet. However, CD could not differentiate between cross-β and β-sheets (Appendix 3).

DISCUSSION

In the present work, we characterized intermediate aggregate species formed on the aggregation pathway of human γD-crystallin protein under a low pH condition. The results indicate that γD-crystallin protein forms pentamer, 25-mer, and higher oligomer intermediates. FCS and FTIR showed that the human γD-crystallin protein undergoes unfolding to form intermediate aggregate species enriched in a random coil structure. The visualization of the same was done by TEM.

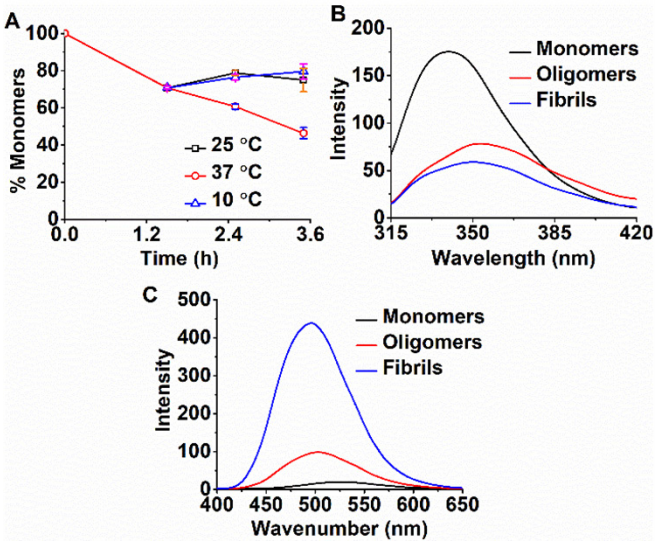

Figure 4. Biophysical characterization of γD-Crystallin aggregation. **A**: Aggregation kinetics of γD-crystallin at different temperatures in pH 2.5. **B**: Tryptophan fluorescence assay of monomers, oligomers, and fibrils. **C**) ANS binding assay of monomers, oligomers, and fibrils.

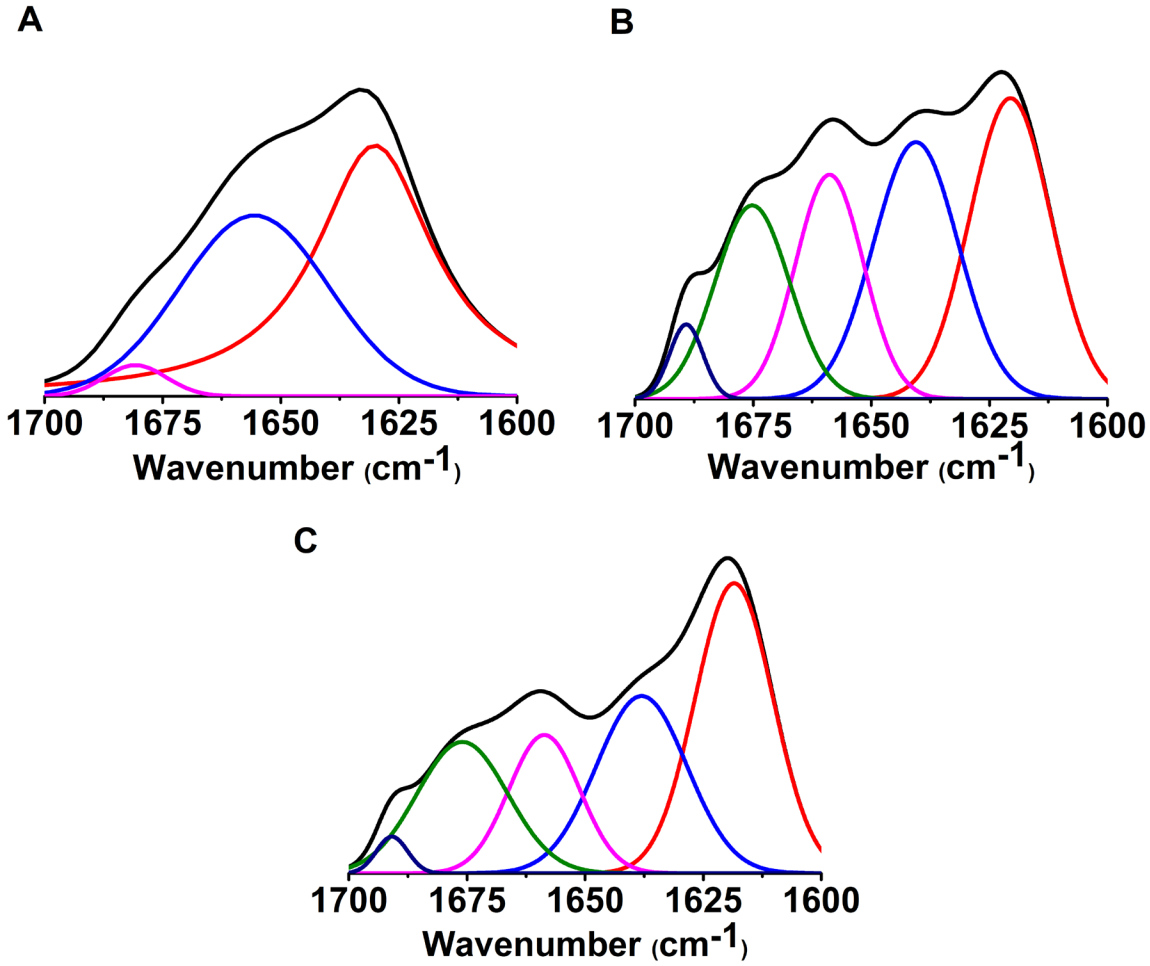

Figure 5. Curve fit fourier-transform infrared spectroscopy (FTIR) spectra of different aggregate species. **A**: Curve-fitted primary spectrum of monomers. **B**: Curve-fitted primary spectrum of oligomers. **C**: Curve-fitted primary spectrum of fibrils. The spectra of all three species differ from one another.

The combination of RP-HPLC sedimentation, light scattering, and ThT binding assays yielded insightful results about the aggregation behavior of γD-crystallin under experimental conditions. The absence of a distinguishable lag phase, a hallmark of conventional amyloid aggregation, suggests an intriguing departure from the norm. The amyloid aggregation process is generally described in three phases: lag phase, growth phase, and plateau phase. Lag phase represents the time required for formation of the nucleus, which further grows in the elongation phase [31]. A prominent lag phase was reported in aggregation kinetics of polyglutamine peptides [32] and insulin [33], whereas no lag phase was reported in N-terminus huntingtin [34] and IAPP [35] peptide fragment aggregation. Thus, γD-crystallin may represent the case of downhill aggregation reaction as observed in the N-terminus huntingtin protein fragment [34]. Further, FCS and analytical ultracentrifugation experiments showed the presence of various intermediate species on the aggregation pathway. From FCS data, it was observed that the radius of the intermediate species formed during the aggregation reaction was gradually increasing as the aggregation progressed (Figure 2A). This indicates the formation of higher-order aggregates as the aggregation time increased. FCS data indicate that on the aggregation pathway of γD-crystallin protein under pH 2.5, an aggregate species constituting approximately 5 ± 0.66 monomers was formed after 3 min (Appendix 1). This might have formed due to the association of five monomeric γD-crystallin protein. However, dimers, trimers, or tetramers may also be present for a short time. Perhaps due to their transient nature, these species were not detected within the

time frame of the FCS experiment. In the process of intermediate aggregating species formation, γD-crystallin monomers are also present in the reaction mixture. Therefore, in the formation of 25-mer species, the possibility of an association of monomers with the 5 ± 0.66-mer species and similarly, for the 110 ± 82-mer species, an association of monomers with 25-mer species, cannot be ignored. Previously, FCS was also used to study the aggregation pathway of other amyloid proteins. In the case of Aβ peptide, the FCS study suggested that the aggregation process starts with the formation of dimer, and further higher aggregates were reported as the aggregation time progressed [36]. Similarly, the formation of early aggregates of α-synuclein protein was also monitored by FCS [37].

The morphologic examination of γD-crystallin aggregation via TEM has provided crucial insights into the progression of aggregate structures. The initial stage of aggregation, marked by the presence of spherical oligomers with a diameter of 10 nm, showcases the early assembly events. Notably, the absence of fibril-like structures at this early stage of the aggregation process suggests that the oligomeric state predominates during this period. Subsequent to the oligomeric phase, the emergence of protofibrils with a width of approximately 7 nm at the 3 h time point signifies a transition toward more organized structures. The morphologic transition from spherical oligomers to these protofibrils suggests an intricate interplay of molecular interactions driving the aggregation process. As the reaction advances, the appearance of larger fibril-like structures at the 5 h and 30 h time points, exhibiting widths of 15 nm and 35 nm, respectively, signifies the maturation of aggregates over time. The observed transformation from oligomers to protofibrils and ultimately to mature fibrils, as depicted in Figure 3, underscores the hierarchical nature of the aggregation process of γD-crystallin. This evolution of morphologic features highlights the progressive organization of the protein molecules into higher-order structures.

The dynamic nature of aggregation intermediates, as revealed by FCS data and TEM analysis, highlights the complexity of the aggregation process and the formation of various species with distinct sizes and shapes. This heterogeneity likely corresponds to diverse biophysical characteristics that may play pivotal roles in the aggregation mechanism. The utilization of tryptophan fluorescence and ANS binding assays to probe conformational changes during aggregation yielded noteworthy results. The red shift in tryptophan fluorescence wavelengths for oligomers and fibrils, accompanied by the blue shift in ANS binding wavelengths, collectively indicates alterations in the protein environment and exposure of previously sequestered hydrophobic regions. These conformational changes are attributed to the transition from the native globular structure to the evolving conformations of oligomers and fibrils. Change in protein conformation was also reported in oligomers of Aβ, α-synuclein, lysozyme, and insulin proteins [38-40]. Change in conformation was also reported during aggregation of γD-crystallin in the presence of GuHCl [41] and UV-C light [42]. All these proteins follow different aggregation pathways and contain various aggregating intermediate structures. Therefore, change in γD-crystallin conformations is an important step in the aggregation pathway, and it may lead to the formation of various intermediate aggregating species.

The intricate interplay between secondary structural changes and the aggregation pathway of γD-crystallin is unveiled through the integration of FTIR spectroscopy and other complementary assays. The presence of cross-β sheet structures in both oligomers and fibrils signifies a commonality in their underlying arrangement, which aligns with the ThT binding assay results and suggests their involvement in amyloid-like aggregates. Oligomers of various amyloid proteins have been reported to possess different types of structural elements. Aβ oligomers in physiologic conditions are rich in β-sheet [40,43]. Similarly, lysozyme oligomers were reported with the presence of cross-β sheet and also rich in unstructured elements [38]. Oligomers of insulin [44] and α-synuclein [45] were reported to be rich in the α-helix structure. In our study, γD-crystallin oligomers were rich in cross-β sheet and unstructured elements, as shown in lysozyme oligomers. Further, it was found that γD-crystallin protein monomers had a different secondary structure at pH 2.5 than at pH 7 (Appendix 3). Under acidic pH, γD-crystallin monomers were observed to be rich in α-helix (1,659 cm^{-1}) rather than β-turn (1,665 cm^{-1}), as reported in pH 7. This change in secondary structure of γD-crystallin protein in acidic pH corroborates with our FCS data, which represent an increase in the size of γD-crystallin protein in pH 2.5. Overall, γD-crystallin protein changes its conformation to form oligomers, which are rich in cross-β sheet, and then later, as the aggregation progresses, protofibrils (as observed in TEM) and fibrils with different secondary structural characteristics are formed.

In this study, for the first time, we have reported the presence of various intermediate aggregate species of γD-crystallin that form at low pH. FCS study shows that aggregation starts with the formation of aggregate species constituting of five monomeric units, which further grow to form 25-mer, 110 ± 82-mer, and bigger oligomers (Figure 6). TEM study indicates γD-crystallin monomers first form

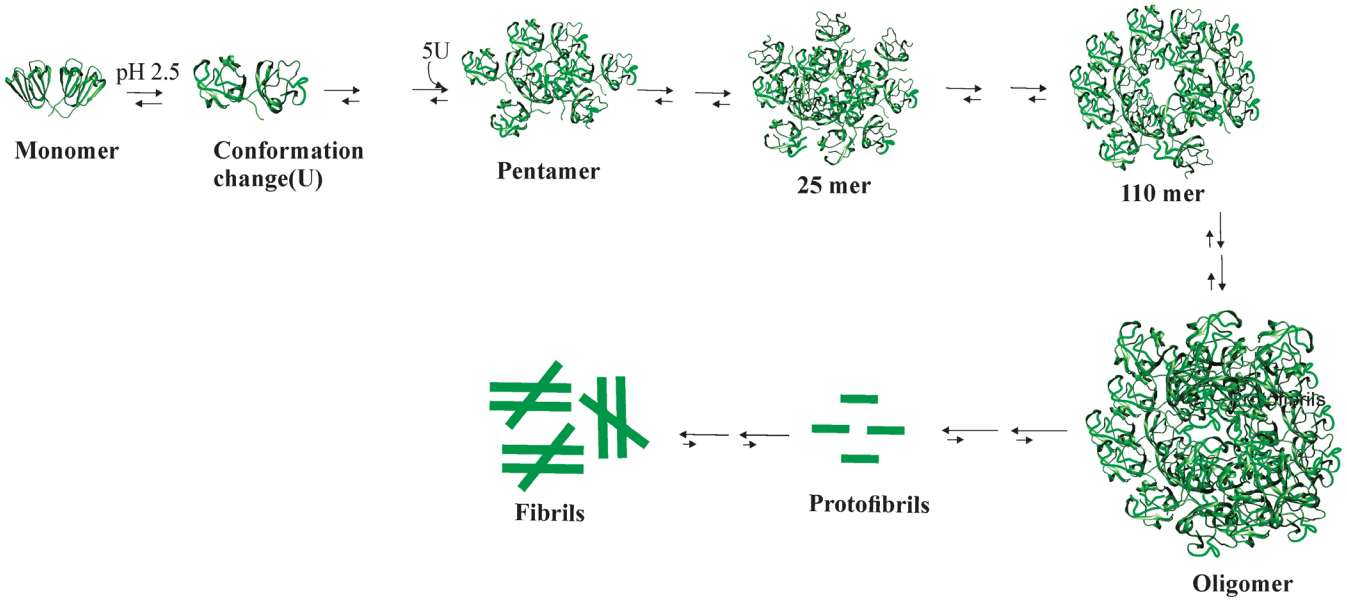

Figure 6. Proposed aggregation pathway for γD-crystallin protein at pH 2.5. The monomer PDB (Protein Data Bank) ID is 1HK0, while all other images are for representative purposes only.

oligomers, which further grow to form protofibrils and then fibrils. FTIR study shows oligomers are rich in cross-β sheet structure. Furthermore, to gain a thorough knowledge of the atomic-level structural features of the fibrils generated, high-resolution techniques like cryo-electron microscopy could be used. This study will open new areas of research in understanding the detailed aggregation mechanism and aggregation hotspot within unfolded γD-crystallin monomers. This will eventually help in designing mechanism-based inhibitors of aggregation in cataract disease.

APPENDIX 1. FCS AUTOCORRELATION AND ANALYTICAL ULTRACENTRIFUGATION OF THE ΓD-CRYSTALLIN PROTEIN IN PH 7.

To access the data, click or select the words "Appendix 1."

APPENDIX 2. TEM AND DLS ANALYSIS OF PROTEIN IN PH 2.5.

To access the data, click or select the words "Appendix 2."

APPENDIX 3. CD SPECTRUM OF MONOMER AND OLIGOMER AT PH 2.5 AND FTIR ANALYSIS OF PROTEIN IN PH 7.

To access the data, click or select the words "Appendix 3."

ACKNOWLEDGMENTS

We would like to thank Prof. Martin Zanni (Department of Chemistry, University of Wisconsin Madi-son, USA) for providing clone of γD crystallin protein, Dr. Saravanan Matheshwaran (Department of Biological Sciences and Bioengineering, Indian Institute of Technology Kanpur, India) for protein purification. Analytical ultracentrifugation facility was provided by Institute of Microbial Technology, India. We acknowledge the Sophisticated Analytical Instrumentation Facility, All India Institute of Medical Sciences New Delhi, India for TEM facility. We thank Nilimesh Das (Department of Chemistry, Indian Institute of Technology Kanpur, India) for helping in FCS graph preparation. Mangesh Bawankar acknowledges Ministry of Human Resource Development and Indian Institute of Technology Kanpur, India for fellowship. Funding Sources: Indian Institute of Technology Kanpur, India (PDAIITK20100293) and Science and Engineering Research Board, Government of India (Grant No. EMR2016006555).

REFERENCES

1. Lam D, Rao SK, Ratra V, Liu Y, Mitchell P, King J, Tassignon MJ, Jonas J, Pang CP, Chang DF. Cataract. Nat Rev Dis Primers 2015; 1:15014-[PMID: 27188414].
2. Morishita H, Mizushima N. Autophagy in the lens. Exp Eye Res 2016; 144:22-8. [PMID: 26302409].
3. Moran SD, Zhang TO, Zanni MT. An alternative structural isoform in amyloid-like aggregates formed from thermally

denatured human γD-crystallin. Protein Sci 2014; 23:321-31. [PMID: 24415662].

4. Zhao L, Chen X-J, Zhu J, Xi Y-B, Yang X, Hu L-D, Ouyang H, Patel SH, Jin X, Lin D, Wu F, Flagg K, Cai H, Li G, Cao G, Lin Y, Chen D, Wen C, Chung C, Wang Y, Qiu A, Yeh E, Wang W, Hu X, Grob S, Abagyan R, Su Z, Tjondro HC, Zhao XJ, Luo H, Hou R, Jefferson J, Perry P, Gao W, Kozak I, Granet D, Li Y, Sun X, Wang J, Zhang L, Liu Y, Yan YB, Zhang K. Lanosterol reverses protein aggregation in cataracts. Nature 2015; 523:607-11. [PMID: 26200341].

5. Arnaudov LN, de Vries R. Thermally induced fibrillar aggregation of hen egg white lysozyme. Biophys J 2005; 88:515-26. [PMID: 15489299].

6. Vernaglia BA, Huang J, Clark ED. Guanidine hydrochloride can induce amyloid fibril formation from hen egg-white lysozyme. Biomacromolecules 2004; 5:1362-70. [PMID: 15244452].

7. Borzova VA, Markossian KA, Chebotareva NA, Kleymenov SY, Poliansky NB, Muranov KO, Stein-Margolina VA, Shubin VV, Markov DI, Kurganov BI. Kinetics of thermal denaturation and aggregation of bovine serum albumin. PLoS One 2016; 11:e0153495[PMID: 27101281].

8. Coles WH, Jaros PA. Dynamics of ocular surface pH. Br J Ophthalmol 1984; 68:549-52. [PMID: 6743624].

9. Eckert R. pH gating of lens fibre connexins. Pflugers Arch 2002; 443:843-51. [PMID: 11889584].

10. Bassnett S, Croghan PC, Duncan G. Diffusion of lactate and its role in determining intracellular pH in the lens of the eye. Exp Eye Res 1987; 44:143-7. [PMID: 3556449].

11. Papanikolopoulou K, Mills-Henry I, Thol SL, Wang Y, Gross AAR, Kirschner DA, Decatur SM, King J. Formation of amyloid fibrils in vitro by human gammaD-crystallin and its isolated domains. Mol Vis 2008; 14:81-9. [PMID: 18253099].

12. Moran SD, Woys AM, Buchanan LE, Bixby E, Decatur SM, Zanni MT. Two-dimensional IR spectroscopy and segmental 13C labeling reveals the domain structure of human γD-crystallin amyloid fibrils. Proc Natl Acad Sci U S A 2012; 109:3329-34. [PMID: 22328156].

13. Moran SD, Decatur SM, Zanni MT. Structural and sequence analysis of the human γD-crystallin amyloid fibril core using 2D IR spectroscopy, segmental 13C labeling, and mass spectrometry. J Am Chem Soc 2012; 134:18410-6. </jrn>[PMID: 23082813].

14. Haass C, Selkoe DJ. Soluble protein oligomers in neurodegeneration: lessons from the Alzheimer's amyloid β-peptide. Nat Rev Mol Cell Biol 2007; 8:101-12. [PMID: 17245412].

15. Fändrich M. Oligomeric intermediates in amyloid formation: structure determination and mechanisms of toxicity. J Mol Biol 2012; 421:427-40. [PMID: 22248587].

16. Glabe CG, Kayed R. Common structure and toxic function of amyloid oligomers implies a common mechanism of pathogenesis. Neurology 2006; 66:Suppl 1S74-8. [PMID: 16432151].

17. Deshpande A, Mina E, Glabe C, Busciglio J. Different conformations of amyloid β induce neurotoxicity by distinct mechanisms in human cortical neurons. J Neurosci 2006; 26:6011-8. [PMID: 16738244].

18. Danzer KM, Haasen D, Karow AR, Moussaud S, Habeck M, Giese A, Kretzschmar H, Hengerer B, Kostka M. Different species of α-synuclein oligomers induce calcium influx and seeding. J Neurosci 2007; 27:9220-32. [PMID: 17715357].

19. O'Nuallain B, Thakur AK, Williams AD, Bhattacharyya AM, Chen S, Thiagarajan G, Wetzel R. Kinetics and thermodynamics of amyloid assembly using a high-performance liquid chromatography-based sedimentation assay. Methods Enzymol 2006; 413:34-74. [PMID: 17046390].

20. Mandal U, Ghosh S, Mitra G, Adhikari A, Dey S, Bhattacharyya K. A femtosecond study of the interaction of human serum albumin with a surfactant (SDS). Chem Asian J 2008; 3:1430-4. [PMID: 18666281].

21. Lowry O, Rosebrough N, Farr A. Randall, RJ Ž. J Biol Chem 1951; 1951:265-75. [PMID: 14907713].

22. Das N, Sen P. Structural, Functional, and Dynamical Responses of a Protein in a Restricted Environment Imposed by Macromolecular Crowding. Biochemistry 2018; 57:6078-89. [PMID: 30264990].

23. Mohan V, Das N, Das A, Mishra V, Sen P. Spectroscopic Insight on Ethanol-Induced Aggregation of Papain. J Phys Chem B 2019; 123:2280-90. [PMID: 30775921].

24. Lakowiz J. Principles of fluorescence spectroscopy. 3^ nd ed. Maryland: Plenum Press; 2006.

25. Müller C, Loman A, Pacheco V, Koberling F, Willbold D, Richtering W. Precise measurement of diffusion by multi-color dual-focus fluorescence correlation spectroscopy. EPL 2008; 83:46001-Europhysics Letters..

26. Ostapchenko VG, Sawaya MR, Makarava N, Savtchenko R, Nilsson KPR, Eisenberg D, Baskakov IV. Two amyloid States of the prion protein display significantly different folding patterns. J Mol Biol 2010; 400:908-21. [PMID: 20553730].

27. Vivian JT, Callis PR. Mechanisms of tryptophan fluorescence shifts in proteins. Biophys J 2001; 80:2093-109. [PMID: 11325713].

28. Hawe A, Sutter M, Jiskoot W. Extrinsic fluorescent dyes as tools for protein characterization. Pharm Res 2008; 25:1487-99. [PMID: 18172579].

29. Ridgley DM, Ebanks KC, Barone JR. Peptide mixtures can self-assemble into large amyloid fibers of varying size and morphology. Biomacromolecules 2011; 12:3770-9. [PMID: 21879764].

30. Kong J, Yu S. Fourier transform infrared spectroscopic analysis of protein secondary structures. Acta Biochim Biophys Sin (Shanghai) 2007; 39:549-59. [PMID: 17687489].

31. Arosio P, Knowles TP, Linse S. On the lag phase in amyloid fibril formation. Phys Chem Chem Phys 2015; 17:7606-18. [PMID: 25719972].

32. Bhattacharyya AM, Thakur AK, Wetzel R. polyglutamine aggregation nucleation: thermodynamics of a highly unfavorable protein folding reaction. Proc Natl Acad Sci U S A 2005; 102:15400-5. [PMID: 16230628].

33. Pease LF 3rd, Sorci M, Guha S, Tsai D-H, Zachariah MR, Tarlov MJ, Belfort G. Probing the nucleus model for oligomer formation during insulin amyloid fibrillogenesis. Biophys J 2010; 99:3979-85. [PMID: 21156140].

34. Thakur AK, Jayaraman M, Mishra R, Thakur M, Chellgren VM, Byeon I-JL, Anjum DH, Kodali R, Creamer TP, Conway JF, Gronenborn AM, Wetzel R. Polyglutamine disruption of the huntingtin exon 1 N terminus triggers a complex aggregation mechanism. Nat Struct Mol Biol 2009; 16:380-9. [PMID: 19270701].

35. Wei L, Jiang P, Xu W, Li H, Zhang H, Yan L, Chan-Park MB, Liu XW, Tang K, Mu Y, Pervushin K. The molecular basis of distinct aggregation pathways of islet amyloid polypeptide. J Biol Chem 2011; 286:6291-300. </jrn>[PMID: 21148563].

36. Tjernberg LO, Pramanik A, Björling S, Thyberg P, Thyberg J, Nordstedt C, Berndt KD, Terenius L, Rigler R. Amyloid β-peptide polymerization studied using fluorescence correlation spectroscopy. Chem Biol 1999; 6:53-62. [PMID: 9889152].

37. Nath S, Meuvis J, Hendrix J, Carl SA, Engelborghs Y. Early aggregation steps in α-synuclein as measured by FCS and FRET: evidence for a contagious conformational change. Biophys J 2010; 98:1302-11. [PMID: 20371330].

38. Frare E, Mossuto MF, de Laureto PP, Tolin S, Menzer L, Dumoulin M, Dobson CM, Fontana A. Characterization of oligomeric species on the aggregation pathway of human lysozyme. J Mol Biol 2009; 387:17-27. [PMID: 19361437].

39. Hua QX, Weiss MA. Mechanism of insulin fibrillation: the structure of insulin under amyloidogenic conditions resembles a protein-folding intermediate. J Biol Chem 2004; 279:21449-60. [PMID: 14988398].

40. Breydo L, Uversky VN. Structural, morphological, and functional diversity of amyloid oligomers. FEBS Lett 2015; 589:19 Pt A2640-8. [PMID: 26188543].

41. Kosinski-Collins MS, King J. In vitro unfolding, refolding, and polymerization of human gammaD crystallin, a protein involved in cataract formation. Protein Sci 2003; 12:480-90. [PMID: 12592018].

42. Wang SSS, Wen W-S. Examining the influence of ultraviolet C irradiation on recombinant human γD-crystallin. Mol Vis 2010; 16:2777-90. [PMID: 21197112].

43. Ma B, Nussinov R. Polymorphic C-terminal β-sheet interactions determine the formation of fibril or amyloid β-derived diffusible ligand-like globulomer for the Alzheimer Abeta42 dodecamer. J Biol Chem 2010; 285:37102-10. [PMID: 20847046].

44. Vestergaard B, Groenning M, Roessle M, Kastrup JS, van de Weert M, Flink JM, Frokjaer S, Gajhede M, Svergun DI. A helical structural nucleus is the primary elongating unit of insulin amyloid fibrils. PLoS Biol 2007; 5:e134[PMID: 17472440].

45. Ghosh D, Singh PK, Sahay S, Jha NN, Jacob RS, Sen S, Kumar A, Riek R, Maji SK. Structure based aggregation studies reveal the presence of helix-rich intermediate during α-Synuclein aggregation. Sci Rep 2015; 5:9228-[PMID: 25784353].